Biomaterials 35 (2014) 6750–6757

Contents lists available at ScienceDirect

Biomaterials

journal homepage: www.elsevier.com/locate/biomaterials

The effects of confinement on neuronal growth cone morphology and velocity

Michael S. Smirnov [a,b], Katelyn A. Cabral [c], Herbert M. Geller [c,1], Jeffrey S. Urbach [b,*,1]

[a] Interdisciplinary Program in Neuroscience, Georgetown University, Washington, DC 20057, USA
[b] Department of Physics and the Institute for Soft Matter Synthesis and Metrology, Georgetown University, 320 Regents Hall, Washington, DC 20057, USA
[c] Developmental Neurobiology Section, Cell Biology and Physiology Center, National Heart, Lung, and Blood Institute, National Institutes of Health, Bethesda, MD 20892, USA

ARTICLE INFO

Article history:
Received 12 March 2014
Accepted 21 April 2014
Available online 16 May 2014

Keywords:
Neural cell
Polyvinylalcohol
Nerve regeneration
Laminin
Laser ablation

ABSTRACT

Optimizing growth cone guidance through the use of patterned substrates is important for designing regenerative substrates to aid in recovery from neuronal injury. Using laser ablation, we designed micron-scale patterns capable of confining dissociated mouse cerebellar granule neuron growth cones to channels of different widths ranging from 1.5 to 12 μm. Growth cone dynamics in these channels were observed using time-lapse microscopy. Growth cone area was decreased in channels between 1.5 and 6 μm as compared to that in 12 μm and unpatterned substrates. Growth cone aspect ratio was also affected as narrower channels forced growth cones into a narrow, elongated shape. There was no difference in the overall rate of growth cone advance in uniform channels between 1.5 and 12 μm as compared to growth on unpatterned substrates. The percentage of time growth cones advanced, paused, and retracted was also similar. However, growth cones did respond to changes in confinement: growth cones in narrow lanes rapidly sped up when encountering a wide region and then slowed down as they entered another narrow region. Our results suggest that the rate of neurite extension is not affected by the degree of confinement, but does respond to changes in confinement.

1. Introduction

Strategies for promoting regeneration following injury to the mammalian central nervous system generally incorporate the use of implantable biomaterials to guide neurons [1–4], with extensive research focusing on the design of various topographic and structural patterns in order to direct neuronal outgrowth [5]. Directed neurite outgrowth has been mainly achieved by patterning surfaces with aligned linear features. In addition, the rate of neurite outgrowth on these patterns can be modulated by altering specific structural parameters of the substrate. For example, dorsal root ganglia (DRG) neurons have been shown to extend farther on protein-coated fibers of smaller diameter [6]. DRGs extending along printed channels of laminin, a known permissive substrate, have also shown a preference for certain channel widths [7,8]. The mechanisms underlying these responses to substrate features are not known.

The growth cone is the structure responsible for integrating chemical and structural signals from the extracellular matrix and controlling neurite extension. Growth cones alter their size as well as rate of movement as a response to pattern dimensions [7,9,10]. However, a detailed understanding of these responses is lacking. We employed a laser ablation technique [11] to fabricate a model system of laminin-coated channels for guiding neurons, allowing us to achieve the micron-scale resolution necessary to alter growth cone morphology. Furthermore, we used dissociated cerebellar granule neurons (CGNs) to better identify isolated effects of growth cone size. The objective of our study was to use high-resolution, time-lapse microscopy on live cells extending on our fabricated patterns to evaluate the relationships between substrate structure and growth cone size, shape, and rate of extension.

2. Materials and methods

2.1. Glass-bottom dish preparation

Dishes were prepared according to a previously published protocol [11]. Briefly, glass-bottom (MatTek) dishes were washed with 50% HNO_3, treated with 200 mM NaOH, rinsed with H_2O, and silanized using 1% triethoxysilylbutraldehyde (Gelest) in ethanol. Surfaces were washed with ethanol and H_2O and allowed to cure for 3 h at 65 °C. A 5.6% PVA solution was prepared by dissolving PVA (molecular

* Corresponding author. Fax: +1 202 687 2087.
E-mail address: urbach@physics.georgetown.edu (J.S. Urbach).
[1] H.M.G. and J.S.U contributed equally to this work.

http://dx.doi.org/10.1016/j.biomaterials.2014.04.097
0142-9612/

weight ≈ 98,000; 98% hydrolyzed; Sigma–Aldrich) in H_2O at 90°C and filtered through a 0.2 μm filter. 2N HCl was added to the filtered PVA at a 1:8 ratio. The mixture was spin-coated onto the silanized glass-bottom dishes at 7000RPM for 45 s and the dishes were stored at 4 °C.

2.2. Photoablation

A Leica SP5 Multi-Photon (dual beam with OPO)/Confocal Microscope was used for photoablation. ROIs were generated using Leica operating software. A 63× NA 1.4 oil immersion objective was used during ablation. Digital zoom was set to 4× in order to decrease amount of z-tilt in the field of view. Autofocus was performed using reflectance from a low power 633 nm laser. Ablation was achieved via a two-photon laser at 800 nm and ≈35% power, scanning at 100 Hz at a 512 × 512 resolution. These settings allowed us to burn away PVA but prevent scorching of the glass surface. Leica MatrixScreener software was used to automate the process in order to create consistent, tiled patterns. To prevent autofluorescence, dishes were quenched for 8 min with 2 ml of 0.5% $NaBH_4$ in 200 mM Ethanolamine buffer (200 mM $EtOHNH_3$, 100 mM NaH_2PO_4, pH 8.0) and then washed 3× with PBS.

2.3. Laminin labeling and attachment

Laminin was conjugated with Alexa Fluor-488 dye (Life Technologies) using supplied protocols. Fluorescently labeled laminin was diluted to 25 μg/ml in PBS with 0.1% Pluronic F-127 (Life Technologies) and added to coverslips for 30 min at room temp. Dishes were washed 3× with PBS and kept in PBS until use.

2.4. Atomic force microscopy (AFM) imaging

Topographic images of the ablated regions were acquired with a Solver Next (NT-MDT) scanning probe microscope operating in oscillating mode.

2.5. Cell culture

Cultures of dissociated mouse CGNs were prepared from postnatal 5-day-old C57BL/6 mice as described previously [12]. Dissociated cells plated on laminin/coated patterns and 2D unpatterned laminin-coated glass dishes in Neurobasal-A medium containing B27 (1:50, v/v) supplement, glutaMAX (1:100, v/v, Life Technologies), Pen/Strep, and 25 mM KCl.

2.6. Scanning electron microscopy (SEM) preparation and imaging

Coverslip cultures were fixed in 2.5% glutaraldehyde, 1% paraformaldehyde, 0.12 M sodium cacodylate buffer, pH 7.3, postfixed with 1% OsO4 in the same buffer, dehydrated in an ethanol series and critical point dried out of CO_2 in a Samdri-795 critical point dryer (Tousimis Research Corp, Rockville MD). The dried coverslip cultures were coated with 5 nm of gold in an EMS 575-X sputter coater (Electron Microscopy Sciences, Hatfield PA) and imaged with a Hitachi S-3400 N1 scanning electron microscope (Hitachi High Technologies America, Inc., Pleasanton CA).

2.7. Time-lapse microscopy

Phase contrast images were obtained using a Nikon Eclipse TE2000-E inverted microscope equipped with a 37 °C and 5%CO_2 incubation chamber, 63× oil objective, and a motorized stage (Prior Scientific). Metamorph software (Molecular Devices) with the multidimensional acquisition plugin was used to capture images and control all hardware. Images were acquired using a 63× oil objective and digital camera (Hamamatsu Photonics). Regular time-lapse imaging was performed in ~20 locations at 5 min intervals over two 24-h periods, while high time-resolution imaging was performed in one location at 5 s intervals. Laminin fluorescence was detected using epifluorescence illumination with a mercury lamp and a 488 nm filter cube.

2.8. Image processing and analysis

Image processing was performed using ImageJ [13]. Image stacks were imported and drift-stabilized using the Template Matching plugin. The MtrackJ plugin was used to track growth cone position, while area and aspect ratio (calculated as a ratio between major and minor axes) were measured by manually tracing each growth cones in each frame. Data analysis was completed using Matlab 2013a (MathWorks).

103 growth cones in were measured on uniform channels and in 2D. The wrist of the growth cone was used as the coordinate for growth cone position. Directionality was determined by setting a reference point at the very beginning of each the channel. For unpatterned 2D controls, the reference point was the first position in frame. Movement toward and away from the reference resulted in a negative and positive velocity, respectively. Error due to turning was negligible in the channels since there was no sideways movement without significant forward or backward displacement. Significant turning was noted and manually corrected for in control growth cones. Average velocity for each axon was calculated as a total displacement between the first and last recorded position divided by elapsed time, and In-group velocities were analyzed for average and standard error.

Area and aspect ratio measured in each frame were first averaged for each individual growth cone. These values were then averaged between all growth cones in each group to avoid bias due to varying sample size. Cumulative probability histograms were plotted using raw instantaneous area measurements.

Instantaneous velocities at each timepoint were calculated as a change in position along the axis of the channel from the previous frame to the following frame divided by time. Growth cones moving at a rate higher than 0.2 μm/min for at least three consecutive frames (15 min) were considered advancing, while velocities above 0.2 μm/min for fewer than three frames and velocities between 0.2 μm/min and −0.2 μm/min were considered paused. Growth cones with velocities less than −0.2 μm/min were considered to be retracting.

33 growth cones were measured on patterns of channels interspersed with circular nodes. Instantaneous velocity was calculated as a displacement along the axis of the channel of growth cones in each consecutive frame divided by time between frames. Directionality was again determined using a reference point. Growth cone position reflects distance to the closest node center. Average velocities and standard errors were calculated for each position. A moving average function (bin = 4) was used to smooth velocity data before plotting. Growth cone areas were also grouped in 1 μm bins and averaged for each position.

2.9. Statistics

Statistical analysis was performed in MATLAB with a multiple comparison test using a one-way ANOVA. Results were considered statistically significant if $p < 0.05$.

3. Results

To examine growth cone responses to precisely defined μm-scale features, we used ROI-guided two-photon laser ablation to remove polyvinyl alcohol (PVA), a hydrophilic polymer resistant to protein and cell adhesion, from glass-bottom dishes (Fig. 1A). This resulted in grooves of exposed glass surrounded by 100 nm-high walls of PVA (Fig. S1); the scale of pattern features was chosen to best approximate the range of CGN growth cone sizes *in vitro*. The substrate was then incubated with 25 μg/ml laminin to support adhesion and growth. Laminin only adhered to glass exposed by the photoablation process, and its concentration remained consistent

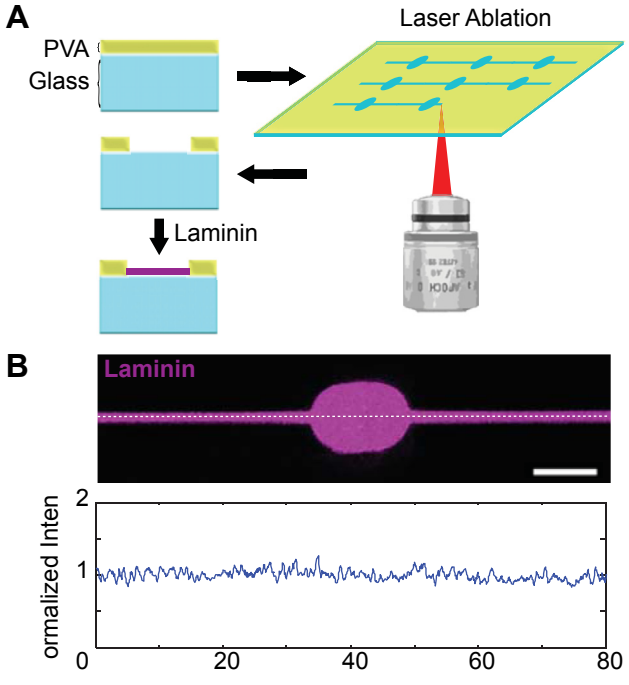

Fig. 1. Generation of laminin-coated patterns using laser photoablation. (A) A thin layer of PVA on top of glass is selectively ablated using repetitive high-power laser scanning in a region of interest. Laminin selectively adheres to glass exposed by the ablation process. (B) AlexaFluor-488 laminin (purple) after adhesion to photoablated dish. Bottom: moving average (bin of 5 pixels) of a fluorescence intensity plot along the white dashed line divided by overall average intensity. Scale bar = 10 μm. (For interpretation of the references to color in this figure legend, the reader is referred to the web version of this article.)